

OPTICAL FIBRES

DOI: 10.1070/QEL16011

Optimisation of an acoustically antiguiding structure for raising the stimulated Brillouin scattering threshold in optical fibres

M.M. Khudyakov, M.E. Likhachev, M.M. Bubnov, D.S. Lipatov, A.N. Gur'yanov, V. Temyanko, J. Nagel, N. Peyghambarian

Abstract. **Optical fibres having a radially nonuniform acoustically antiguiding structure produced by codoping their core with alumina and germania have been fabricated and investigated. The influence of the shape of the antiguiding acoustic refractive index profile and fibre core diameter on the stimulated Brillouin scattering (SBS) threshold and spectrum in the fibres has been assessed. An increase in SBS threshold by 4.4 dB with respect to a germanosilicate fibre having the same mode field diameter has been demonstrated.**

Keywords: *SBS, optical fibre, acoustically antiguiding structure.*

1. Introduction

Stimulated Brillouin scattering (SBS) is a major factor limiting the peak (or average) power of narrow-band (less than 100 MHz in linewidth) fibre lasers and amplifiers. To date, a number of methods for raising the SBS threshold have been proposed. In most of these methods, the acoustic properties of an optical fibre are varied along its length using longitudinal concentration [1–4], temperature [5], or tensile strain [6] gradients. It is worth noting that these methods are often difficult to implement or cannot be used at all (e.g. in the case of relatively short fibres). In this context, considerable attention has been paid to the possibility of producing longitudinally uniform fibres with an increased SBS threshold.

It was shown as early as 1979 that the presence of a waveguide structure not only for light but also for acoustic waves in optical fibres leads to an increase in the time of interaction between an optical and an acoustic mode and, as a consequence, to narrowing of the SBS spectrum [7]. At the same time, according to later theoretical studies, adjusting the acoustic properties of the waveguide allows the SBS bandwidth to be increased, thereby raising the SBS threshold [8–10]. This conclusion is inferred from the fact that an acoustically antiguiding structure leads to acoustic mode leakage to the fibre cladding and a decrease in the time of interaction between the optical and acoustic modes. Practical implementation of such structures became possible owing to the use of alumina, the only dopant that raises the optical refractive index of silica and reduces its acoustic refractive index (doping with alumina increases the speed of sound) [11]. As shown in a number of experimental studies, SBS in alumina-doped fibres can be suppressed by 3–11 dB [12–17].

The presence of an antiguiding acoustic refractive index profile is however insufficient for SBS suppression. In particular, Zou et al. [18] investigated fibres with a reflective fluorosilicate cladding and a slightly fluorinated or pure silica core. Since fluorine reduces the optical refractive index of silica and raises its acoustic refractive index, such fibres are acoustically antiguiding. At the same time, the SBS bandwidth and threshold in them are identical to those in a germanosilicate fibre with similar optical parameters. Moreover, as shown earlier [19] the use of aluminosilicate fibres with a uniform doping profile across the fibre core is incapable of increasing the SBS bandwidth at realistic waveguide parameters (according to estimates, a substantial increase in SBS bandwidth is possible when the working wavelength is twice the cutoff wavelength, but bend sensitivity is then too high). It is worth noting that, in the above-mentioned studies, rather complex, three-layer fibre profiles were often used for SBS suppression, but data necessary for reproducing experiments with such structures (exact dopant profile across the fibre and guiding parameters) were not presented, and in a number of reports [13, 17] even the fibre design was not described.

The purpose of this work was to identify factors responsible for the increased SBS threshold in fibres with an antiguiding acoustic refractive index profile. Optimising the doping profile across the fibre core, we were able to considerably raise the SBS threshold (by more than 3 dB). This effect was shown to occur only at certain guiding parameters of the fibres.

2. Design optimisation for a fibre with an antiguiding acoustic refractive index profile

A detailed analysis of previous work [12–17] indicates that SBS suppression was achieved by using a complex acoustic structure: an additional reflective cladding with a high acoustic refractive index between the fibre core and undoped silica cladding [12, 14–16]. Moreover, according to a num-

M.M. Khudyakov Fiber Optics Research Center, Russian Academy of Sciences, ul. Vavilova 38, 119333 Moscow, Russia; Moscow Institute of Physics and Technology (State University), Institutskii per. 9, 141700 Dolgoprudnyi, Moscow region, Russia;
M.E. Likhachev, M.M. Bubnov Fiber Optics Research Center, Russian Academy of Sciences, ul. Vavilova 38, 119333 Moscow, Russia; e-mail: likhachev@fo.gpi.ru;
D.S. Lipatov G.G. Devyatykh Institute of Chemistry of High-Purity Substances, Russian Academy of Sciences, ul. Tropinina 49, 603950 Nizhnii Novgorod, Russia; Lobachevsky State University of Nizhnii Novgorod, prosp. Gagarina 23, 603950 Nizhnii Novgorod, Russia;
A.N. Gur'yanov G.G. Devyatykh Institute of Chemistry of High-Purity Substances, Russian Academy of Sciences, ul. Tropinina 49, 603950 Nizhnii Novgorod, Russia;
V. Temyanko, J. Nagel, N. Peyghambarian College of Optical Sciences, University of Arizona, 1630 East University Blvd., Tucson, AZ 85721, USA

Received 29 December 2015
Kvantovaya Elektronika **46** (5) 468–472 (2016)
Translated by O.M. Tsarev

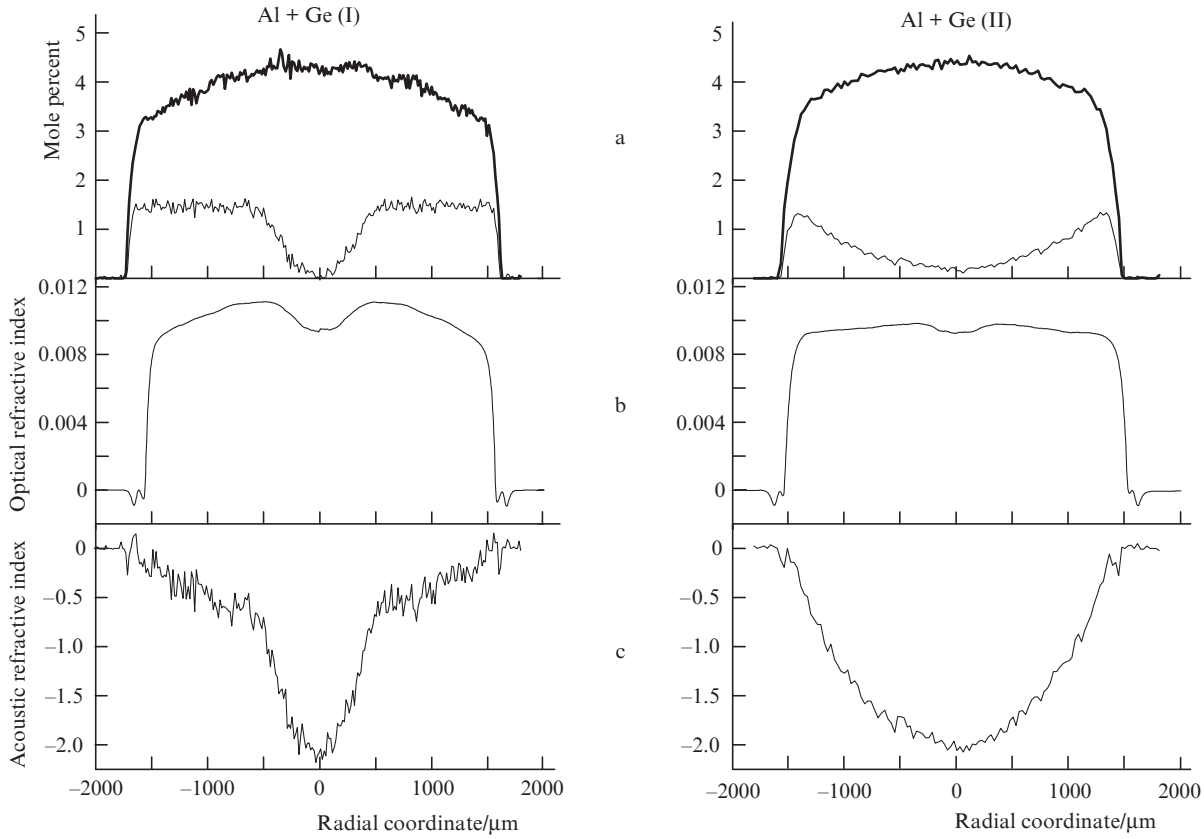

Figure 1. (a) Doping profiles obtained by electron microscopy (Al_2O_3, heavy lines; GeO_2, thin lines) and (b) optical and (c) acoustic refractive index profiles across preforms I (left) and II (right).

ber of reports, a so-called triangular antiguiding acoustic refractive index profile (with the acoustic refractive index decreasing linearly with decreasing distance to the fibre axis, at a constant optical refractive index) should be used for more effective SBS suppression [16, 17, 20, 21]. It is worth noting that, even when the core of a fibre was reported to be uniformly doped [13, 18], the actual doping profile might have a gradient because of the large alumina diffusion coefficient (see, e.g., the refractive index profile of an aluminosilicate fibre in Ref. [15]). Thus, it is reasonable to assume that the failure to suppress SBS gain in previous studies [18, 19] was the result of a uniform doping profile across the fibre core.

To check this assumption in this study, two fibre preforms were produced by MCVD. Both were codoped with alumina and germania so as to produce a nonuniform antiguiding acoustic refractive index profile across the preforms. The preforms differed in the shape of the acoustic refractive index profile. In one preform (I), the acoustic refractive index decreased slowly in the peripheral part and rapidly near the axis ('concave' triangular index profile). By contrast, in the other preform (II) the acoustic refractive index decreased rapidly in the peripheral part of the core and slowly near the preform axis ('convex' triangular index profile). The germania and alumina concentrations at the core–cladding interface were chosen so that the acoustic refractive index was equal to that of undoped silica glass. Figure 1 shows the alumina and germania doping profiles and the optical and acoustic refractive index profiles (calculated as described by Dragic et al. [12]) across the preforms.

Table 1. Characteristics of the fibres, measured SBS threshold and Brillouin gain coefficient evaluated by a direct method (g_B^1) and from the measured threshold (g_B^2).

Fibre designation and outer diameter	$\Delta n/10^{-3}$*	Mode field diameter/μm	SBS threshold I_{th}/mW μm^{-2}			$g_B^1/10^{-12}$ m W^{-1}	$g_B^2/10^{-12}$ m W^{-1}
			min	max	(min + max)/3		
SMF-28	5.5	10.4	40.1	38.5	26.2	13.6	16.0
P	11	7.20	64.3	69.6	44.63	9.6	9.4
Al	8.5	7.83	59.8	74.2	44.67	7.8	9.4
Ge	8.2	8.82	38.3	40.9	26.4	13.8	15.9
Al + Ge (I), 100 μm	10	8.76	82.2	85.3	55.83	5.6	7.5
Al + Ge (I), 125 μm		7.93	64.9	78.4	47.77	7.3	8.8
Al + Ge (II), 100 μm	9.5	10.09	99.7	117.1	72.27	4.4	5.8

* At a wavelength of 1550 nm.

The preforms were drawn into three fibres: from preform I, we obtained two fibres, with outer diameters of 100 and 125 μm; from preform II, we obtained one fibre, with an outer diameter of 100 μm. For comparison, we also used aluminosilicate (Al), phosphosilicate (P) and germanosilicate (Ge) fibres with uniform doping profiles across their cores and a pure silica cladding. The reference fibre used was the standard fibre SMF-28. The characteristics of all the fibres are summarised in Table 1.

3. SBS gain spectra

SBS spectra were measured by a direct method [10] using the setup schematised in Fig. 2. The signal from a single-frequency laser diode (D1) was amplified by an erbium-doped fibre amplifier (EA) and coupled into the test fibre (TF) through a circulator (C). In the opposite direction, a probe beam from a low-power frequency-dithered single-frequency laser diode (D2) was launched through an optical isolator (ISO) and polarisation controller (PC). The output frequency of D2 was varied using a sawtooth pump current. The current-dependent frequency shift was precalibrated. The amplified signal was sent to a photodetector (PD). One advantage of this method is that the Brillouin gain coefficient can be measured directly.

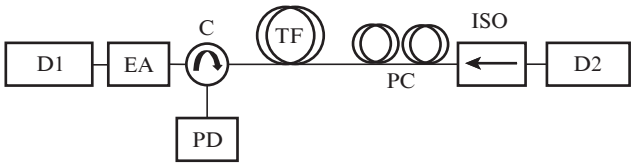

Figure 2. Schematic of the setup used to measure SBS spectra.

Note, however, that the gain coefficient depends on the pump polarisation with respect to the frequency-swept probe beam polarisation (the output of the laser diodes was linearly polarised). Thus, varying the probe beam polarisation, we can obtain a minimum or maximum gain. If only polarisation-maintaining fibres were used in this setup, the minimum gain would be zero (at orthogonal planes of polarisation of the probe and pump beams) and the maximum gain (the planes of polarisation coincide) would be g_B (g_B is the Brillouin gain coefficient when the pump and probe beams are linearly polarised in the same plane). However, if polarisation is not maintained, various external factors (fibre bends, mechanical stress and others) lead to variations in the polarisation state along the length of the fibre. For this reason, the difference between the minimum and maximum gain coefficients measured (using a polarisation controller) at different polarisation states of the pump light and probe signal is smaller: the minimum gain is $^1/_3 g_B$ and the maximum gain is $^2/_3 g_B$ [22]. Thus, the gain coefficient for a linear polarisation can be found by adding up the measured spectra corresponding to the minimum and maximum gains.

The spectra obtained in this study are presented in Fig. 3. It is seen that the spectra of the fibres having no acoustically antiguiding structure (P, Al, Ge, SMF-28) have one, well-defined peak, whereas the spectra of the fibres under investigation (Al + Ge, I and II) have two, comparable peaks, which are due to the interaction of the optical mode with the acoustic modes of the core and cladding [23, 24]. It can be seen that the broadening of the SBS spectrum is accompanied by a decrease in maximum gain. In particular, the maximum coefficients in the Al + Ge (II, 100 μm), Al + Ge (I, 100 μm) and Al + Ge (II, 125 μm) fibres, with a nonuniform acoustically antiguiding structure, were 4.4, 5.6 and 7.3 pm W^{-1}, respectively. At the same time, the maximum gain coefficients of the fibres with a uniform doping profile across their core were 13.8, 13.6, 9.6 and 7.8 pm W^{-1} in Ge, SMF-28, P and Al, respectively. Thus, the SBS gain coefficient in the best fibre, Al + Ge (II, 100 μm), is a factor of 3.1 lower than that in the standard fibre SMF-28.

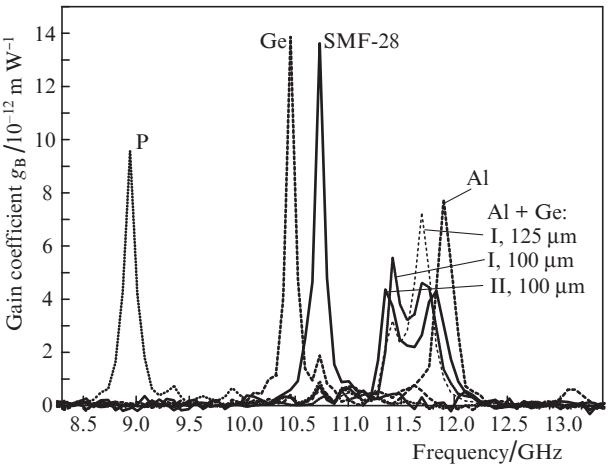

Figure 3. SBS spectra.

4. SBS threshold measurement

Figure 4 shows a schematic of the setup for SBS threshold measurements. The signal source used was a laser diode emitting at a wavelength of 1555 nm. We used two erbium-doped fibre amplifiers with a pump wavelength of 1460 nm (EA1 and EA2) and one with a pump wavelength of 980 nm (EA3).

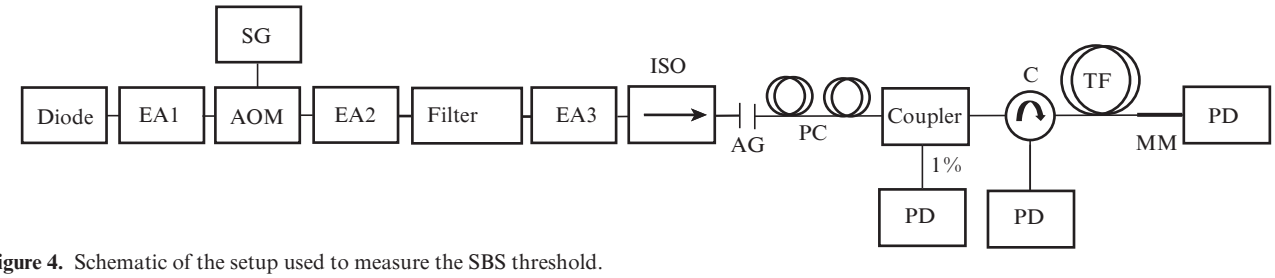

Figure 4. Schematic of the setup used to measure the SBS threshold.

Pulses of 500 ns duration, with a repetition rate of 2 kHz, were cut from the diode signal after the EA1 amplifier using an acousto-optic modulator (AOM) connected to a signal generator (SG). Next, luminescence and the unabsorbed pump light were completely eliminated by a narrow-band filter with a passband of ~1 nm at 1555 nm. After amplification in EA3 to a peak power of 30 W, the resultant signal was launched into the test fibre (TF) through an optical isolator (ISO), air gap (AG) with a variable separation between the facets, polarisation controller (PC), fibre coupler and circulator (C).

The shape of the signal that controlled the acousto-optic modulator was adjusted so that the AOM had a nearly square-wave output signal (Fig. 5). This was, however, only possible at fixed pump powers of the first and second amplifiers. In view of this, an air gap with a variable separation between the fibre facets was used to control the power at the input of the test fibre. To prevent back reflection from the output fibre end, a segment of a multimode (MM) fibre (60/125 μm) was fusion-spliced to it. The SBS signal was detected using a circulator. The signal power coupled into the fibre was determined at the 1% port of the coupler. The SBS threshold was measured for 50-m lengths of the fibres. It is worth noting that the spatial length of 500-ns pulses is about 100 m. Thus, the measured threshold corresponds to a threshold that would be determined in continuous mode at an average power equal to the peak pulse power. The threshold was thought to be reached when the backscattered signal exceeded 1% of the power launched into the fibre.

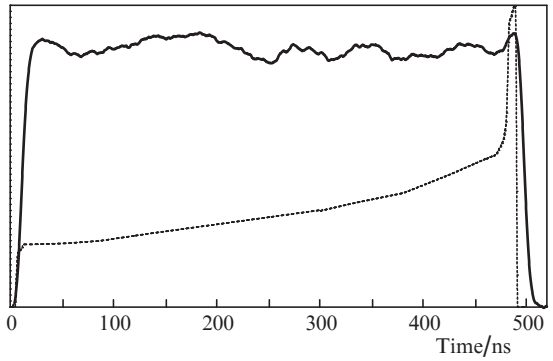

Figure 5. Drive signal shape (dashed line) and light pulse shape (solid curve).

As mentioned above, the SBS threshold depends on pump and probe polarisations. In the case under consideration, the minimum threshold I_{th} is reached at a linear light polarisation, and the maximum threshold ($2I_{th}$), at a circular polarisation. Like in the above case, as a result of uncontrolled birefringence in the test fibre, polarisation varies along the length of the fibre. This fact can be taken into account by introducing a factor x ($0 < x < 0.5$) that corresponds to light 'depolarisation' in the test fibre. Thus, the maximum threshold (nearly circular polarisation) corresponds to $I_{max} = (2 - x)I_{th}$, and the minimum threshold (nearly linear polarisation), to $I_{min} = (1 + x)I_{th}$, where I_{th} is the threshold for a linear polarisation. The measured thresholds were used to evaluate the gain coefficient as [25]

$$g_B = \frac{21}{lI_{th}} = \frac{21}{l(I_{min} + I_{max})/3},$$

where $l = 50$ m is the length of the fibres.

As an example, Fig. 6a shows typical plots of the backscattered signal against pump power density for the Ge fibre. The data were obtained at two positions of the polarisation controller, which ensured the maximum and minimum SBS thresholds. Also presented in Fig. 6a are estimation results for linearly (heavy line) and circularly (dashed line) polarised light. Figure 6b shows estimation results for linearly polarised light in all the fibres. It should be emphasised that, plotting the launched light intensity on the horizontal axis, we exclude the influence of the mode field diameter in the fibre on the comparison results. This is easy to check by comparing the thresholds for the Ge and SMF-28 fibres, which have germania-doped cores and differ in core–cladding refractive index contrast and mode field area by almost a factor of 1.5. Nevertheless, these fibres have essentially identical SBS thresholds.

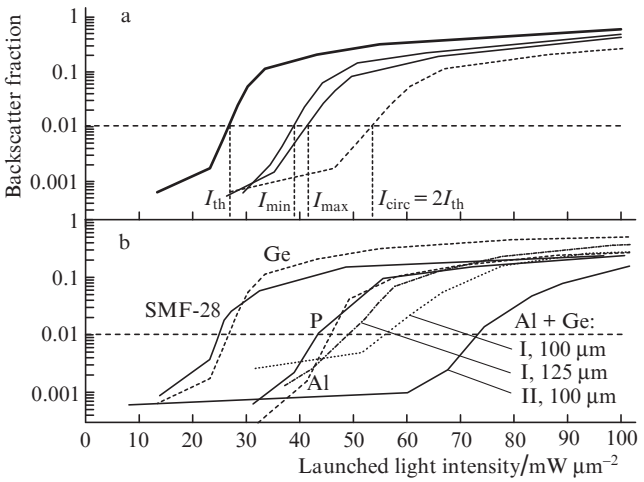

Figure 6. Backscattered signal as a function of power density in the fibre core: (a) measurements at two extreme positions of the polarisation controller (solid lines) and estimation results for linearly (heavy line) and circularly (dashed line) polarised light; (b) estimation results for linearly polarised light in all the fibres.

The estimated maximum SBS gain coefficient is identical to the gain coefficient determined by more accurate, direct measurements (see Section 3) and demonstrates that the uncertainty in SBS threshold calculation from the gain coefficient and that in the inverse calculation may reach 10% to 20%.

The fibres with a uniformly doped core, namely, the phosphosilicate and aluminosilicate fibres (which formally have an antiguiding acoustic refractive index profile), have essentially identical SBS thresholds, near 53.6 mW μm^{-2}, which is a factor of 1.7 greater than the threshold in the germanosilicate fibres: ~31.5 mW μm^{-2}. The SBS threshold in the fibres with a nonuniform acoustic refractive index profile is considerably higher: 57.3 [Al + Ge (I, 125 μm)], 67.0 [Al + Ge (I, 100 μm)] and 86.7 mW μm^{-2} [Al + Ge (II, 100 μm)]. Thus, the maximum increase in the SBS threshold with respect to that in the standard fibre SMF-28 is 4.4 dB. Note that the mode field diameter in the Al + Ge (II, 100 μm) fibre at $\lambda = 1550$ nm is equal to that in SMF-28, so this fibre can be successfully used to replace SMF-28 in SBS-sensitive applications.

5. Discussion and conclusions

The SBS spectra obtained in this study for a variety of optical fibres, with a waveguide structure and an acoustically anti-

guiding structure, demonstrate that a uniform doping profile across the fibre core is incapable of substantially raising the SBS threshold even in a fibre with an antiguiding acoustic refractive index profile (aluminosilicate fibre). To ensure effective SBS suppression in aluminosilicate fibres, the cutoff wavelength should be a factor of 3 shorter than the working wavelength, which leads to high bend sensitivity of such fibres [19]. At the same time, the radially nonuniform antiguiding acoustic refractive index profile produced by codoping with alumina and germania has made it possible to markedly raise the SBS threshold: by about three times. It is important to note that the 'concave' triangular acoustic refractive index profile (preform I) has turned out to be less effective in SBS suppression in comparison with the 'convex', nearly parabolic profile. This finding correlates with theoretical calculations aimed at optimising the acoustic refractive index profile [20]. Even though it has already been pointed out that SBS suppression is possible in fibres with a triangular antiguiding profile [16, 17, 20, 21], this study has been the first to demonstrate that a nonuniform acoustic refractive index profile is a necessary condition for raising the SBS threshold. Moreover, even in this case effective SBS suppression can only be achieved at certain guiding parameters of fibres because the SBS spectrum is strongly dependent on the fibre core diameter. We have demonstrated an increase in SBS threshold by 4.4 dB with respect to that of the germanosilicate fibre SMF-28, which has the same mode field diameter.

Acknowledgements. We are grateful to E.M. Dianov and S.L. Semjonov for their support of and continuous interest in this work.

This study was supported by the Russian Foundation for Basic Research (Grant No. 15-38-20923).

References

1. Takahashi M., Tadakuma M., Hiroishi J., Yagi T. *Proc. ECOC 2007* (Berlin, 2007) paper P014.
2. Tateda M., Ohashi M., Shiraki K. *Proc. OFC* (San Jose, 1993) paper ThJ4.
3. Achmetshin U.G., Bubnov M.M., Guryanov A.N., Dianov E.M., Khopin V.F., Sysoliatin A.A., LiM.-J., Li S., Nolan D.A. *Proc. ECOC 2005* (Glasgow, 2005) paper OFH5.
4. Nagel J., Temyanko V., Dobler J., Salganskii M., Likhachev M., Alexeev V., Bubnov M., Dianov E. , Norwood R., Peyghambarian N. *IEEE Photon. Conf*. (Bellevue, 2013) pp 271 – 272.
5. Liu A. *Opt. Express*, **15**, 977 (2007).
6. Rothenberg J.E., Thielen P.A., Wickham M., Asman C.P. *Proc. SPIE Int. Soc. Opt. Eng*., **6873**, 68730O (2008).
7. Thomas P.J., Rowell N.L., van Driel H.M., Stegeman G.I. *Phys. Rev. B*, **19**, 4986 (1979).
8. Zel'dovich B.Ya., Pilipetskii A.N. *Kvantovaya Elektron.*, **15** (6), 1297 (1988) [*Sov. J. Quantum Electron*., **18** (6), 818 (1988)].
9. Dianov E.M., Karasik A.Ya., Luchnikov A.V., Pilipetskii A.N. *Kvantovaya Elektron*., **16** (4), 752 (1989) [*Sov. J. Quantum Electron*., **19** (4), 491 (1989)].
10. Koyamada Y., Sato S., Nakamura S., Sotobayashi H., Chujo W. *J. Lightwave Technol*., **22**, 631 (2004).
11. Jen C.-K., Neron C., Shang A., Abe K., Bonnel L., Kushibiki J. *J. Am. Ceram. Soc*., **76**, 712 (1993).
12. Dragic P.D., Liu C.H., Papen G.C., Galvanauskas A. *Conf. Lasers and Electro-Optics* (Baltimore, 2005) p. CThZ3.
13. Dragic P.D. In: *2006 Digest LEOS Summer Topical Meeting* (Quebec, 2006) pp 3, 4.
14. Nakanishi T., Tanaka M., Hasegawa T., Hirano M., Okuno T., Onishi M. *Proc. ECOC 2006* (Cannes, 2006) Vol. 6, paper Th. 4.2.2.
15. Li M.J., Chen X., Wang J., Gray S., Liu A., Demeritt J.A., Ruffin A.B., Crowley A.M., Walton D.T., Zenteno L.A. *Opt. Express*, **15** (13), 8290 (2007).
16. Mermelstein M.D., Andrejco M.J., Fini J., Yablon A., Headley C., DiGiovanni D.G., McCurdy A.H. *Proc. SPIE Int. Soc. Opt. Eng*., **6873**, 68730N (2008).
17. Mermelstein M.D. *Opt. Express*, **17**, 16225 (2009).
18. Zou W., He Z., Hotate K. *Opt. Express*, **16**, 18804 (2008).
19. Likhachev M.E., Alekseev V.V., Bubnov M.M., Yashkov M.V., Vechkanov N.N., Gur'yanov A.N., Peyghambarian N., Temyanko V., Nagel J. *Kvantovaya Elektron*., **44** (11), 1043 (2014) [*Quantum Electron*., **44** (11), 1043 (2014)].
20. Nanii O.E., Pavlova E.G. *Kvantovaya Elektron.*, **39** (8), 757 (2009) [*Quantum Electron.*, **39**, 757 (2009)].
21. Villafranca A., Lázaro J.A., Salinas I., Garcés I. *Opt. Express*, **13**, 7336 (2005).
22. van Deventer M.O., Boot A.J. *J. Lightwave Technol*., **12**, 585 (1994).
23. Yoo S., Codemard C.A., Jeong Y., Sahu J.K., Nilsson J. *Appl. Opt*., **49**, 1388 (2010).
24. Dragic P.D. *Proc. SPIE Int. Soc. Opt. Eng*., **7195**, 71952L-1 (2009).
25. Smith R.G. *Appl. Opt*., **11**, 2489 (1972).